Journal of Ceramic Processing Research. Vol. 26, No. 1, pp. 66~75 (2025)
(Received 27 September 2024, Received in revised form 29 November 2024, Accepted 10 January 2025)
https://doi.org/10.36410/jcpr.2025.26.1.66

J O U R N A L O F
Ceramic Processing Research

Process optimization for enhancing the strength properties of celadon body with spherical α-Al_2O_3 powder

Lu Xiong[a,b,*], Yanting Zhong[a], Dong Yao[a], Xianlv Wang[a], Fang Tao[a] and Qijiang Li[a,b]
[a]*Research Centre of Ancient Ceramic, Jingdezhen Ceramic University, Jingdezhen 333001, China*
[b]*Collaborative Innovation Centre for Protection of Ceramic Cultural Relics and Imperial Kiln Study in Jiangxi, Jingdezhen 333001, China*

Longquan celadon, a highly esteemed traditional Chinese ceramic, faces considerable challenges in adapting to modern demands due to its intrinsic brittleness. This study investigates the incorporation of spherical α-Al_2O_3 powder as a reinforcing agent aimed at enhancing the mechanical properties of celadon bodies.By optimizing parameters such as particle size, additive quantity, median diameter of the body material, and firing temperature, a composite material was formulated consisting of 17% 10 μm α-Al_2O_3 with a median diameter (D50) of 2.957 μm. Upon firing at 1310 °C, the modified body demonstrated an average flexural strength of 126.9 MPa, reflecting an impressive improvement of 134% compared to the unoptimized body. Microstructural analyses conducted through Scanning Electron Microscopy (SEM), Energy Dispersive Spectroscopy (EDS), and X-Ray Diffraction (XRD) revealed a network-like distribution of fine corundum grains alongside elongated mullite columns at quartz interfaces. The findings indicate that meticulously calibrated ratios of toughening agents and precise process controls can significantly elevate the performance characteristics of Longquan celadon, making it more suitable for modern industrial applications as well as everyday use.

Keywords: Longquan celadon, α-Al_2O_3 powder, Mechanical properties enhancement, High-temperature firing, Microstructural analysis.

Introduction

As a treasured gem of traditional Chinese ceramic art, Longquan celadon boasts a rich cultural heritage that merits thorough exploration. During the Southern Song Dynasty, Longquan celadon achieved remarkable heights by capitalizing on abundant local natural resources and leveraging porcelain-making techniques from other kilns, successfully producing notable varieties such as pink green and plum green. This period marked its zenith in craftsmanship. Characterized by its unique aesthetic appeal, Longquan celadon has attracted significant attention and scholarly research both domestically and internationally [1-3]. To reignite the brilliance of Longquan celadon, it is essential to harness the collaborative efforts of experts, scholars, and artisans involved in celadon production. Following Premier Zhou's directive that "the five famous kilns, particularly Longquan celadon, must be restored without delay," production resumed at the Longquan Porcelain Factory in Zhejiang Province and Yixing Celadon Factory in Jiangsu Province in 1958. After decades of development, Longquan celadon has once again emerged with renewed glory [4-6].

*Corresponding author:
Tel : 86-13607987434
Fax: 86-13607987434
E-mail: x_lu1986@sina.com

However, as living standards improve, new functional requirements for traditional celadon have emerged. The issue of low strength in celadon significantly hampers the expansion of its product market, particularly during transportation, use, and cleaning processes where collisions can lead to unnecessary losses. In recent years, several scholars [7-13] have conducted in-depth explorations and research into the modification of raw materials and the reinforcement of Longquan celadon's body. For instance, by incorporating talc into the Na_2O-MgO-Al_2O_3-SiO_2 system while utilizing feldspar as a flux, it is possible to produce magnesia-reinforced ceramics that exhibit high strength and good transparency, all while effectively controlling the quantity of high-temperature liquid phase in the body. Additionally, high alumina reinforced ceramics with excellent thermal stability and elevated strength were produced through the introduction of α-Al_2O_3 alongside kaolin, feldspar, and alumina. Furthermore, self-toughened alumina ceramics employing a Li_2O_3-MgO-SiO_2 composite system were developed to achieve an enhancement in flexural strength, Qu Haixia and others characterized and compared the microstructure and mechanical properties of amorphous Al_2O_3 and α-Al_2O_3, finding that under the influence of multiple factors, the composite materials of α-Al_2O_3 have relatively higher bending strength [14]; Ahmet Akkus prepared composite materials by

adding mullite to porcelain in different proportions, finding significant effects on the relative density, microstructure, and phase composition of the composite materials [15]. Some scholars conducted various tests and experiments on alumina, studying its properties. For instance, Zongfu Chu and others explored the effect of alumina fiber content on the viscosity of the slurry and the porosity, phase composition, microstructure, and mechanical properties of the ceramics produced, noting that the fracture toughness increases continuously with the increase of alumina fiber content [16]. Chen Wei and others used various analytical testing methods to study the phase transition rules of alumina during calcination and the evolution of its microstructure [17]. Zhao Dandan focused on the application of alumina in high-performance composite materials for fitness equipment, exploring the reinforcing effect of alumina in composite materials [18]. Hyun Woo Choi studied the effects of Al_2O_3 on the formation of nanocrystals and the crystallization dynamics in glass systems, finding that it changes the crystallization mechanism, affects the activation energy, reduces the nucleation rate, and suppresses crystallization [19].

Considering this, through an analysis and review of relevant literature, this study examines the impact of process parameter optimization on the flexural strength of Longquan celadon bodies. Concurrently, the introduction of α-Al_2O_3 and specific control measures for process parameters are employed to conduct a comprehensive analysis of the enhancements brought about by these parameters on the flexural properties of ceramic samples. The objective of this study is to provide a theoretical foundation and reference for optimizing both production processes and performance characteristics related to Longquan celadon. This endeavor aims to foster development and innovation within Longquan celadon production, which holds significant importance for preserving and protecting the cultural heritage of the Chinese nation while enhancing the competitiveness of ceramic products.

Experimental

Raw materials and process flow

Using Baoxi porcelain clay, potash feldspar, Malaysian kaolin and bentonite as the primary raw materials, samples of Longquan celadon body were prepared utilizing a laboratory simulation method based on the experimental process illustrated in Fig. 1. Table 1 provides a detailed account of the chemical compositions of the various raw materials.

Performance characterization and testing

The sample strips were prepared using an electric powder tablet machine (DY-30, Tianjin Keqi Company, China) with a pressure setting of 4 MPa and a holding time of 10 seconds. Following preparation, the sample strips underwent high-temperature firing prior to strength performance analysis. After high-temperature firing, the samples were evaluated using a universal testing machine (CMT4104, Shandong Wanchen Company, China), and flexural strength data were obtained through analysis software.

Subsequently, the strips were etched with HF acid (5% HF + 95% water) for 20 seconds in an environment maintained at approximately 25 °C. Upon completion of the etching process, the pores and surface roughness of the samples were examined using a super depth-of-field 3D digital microscope (VHX-6000, KEYENCE, Japan). Concurrently, the microstructure and morphology of the samples were analyzed via field emission scanning electron microscopy (SU-8010, HITACHI, Japan), while

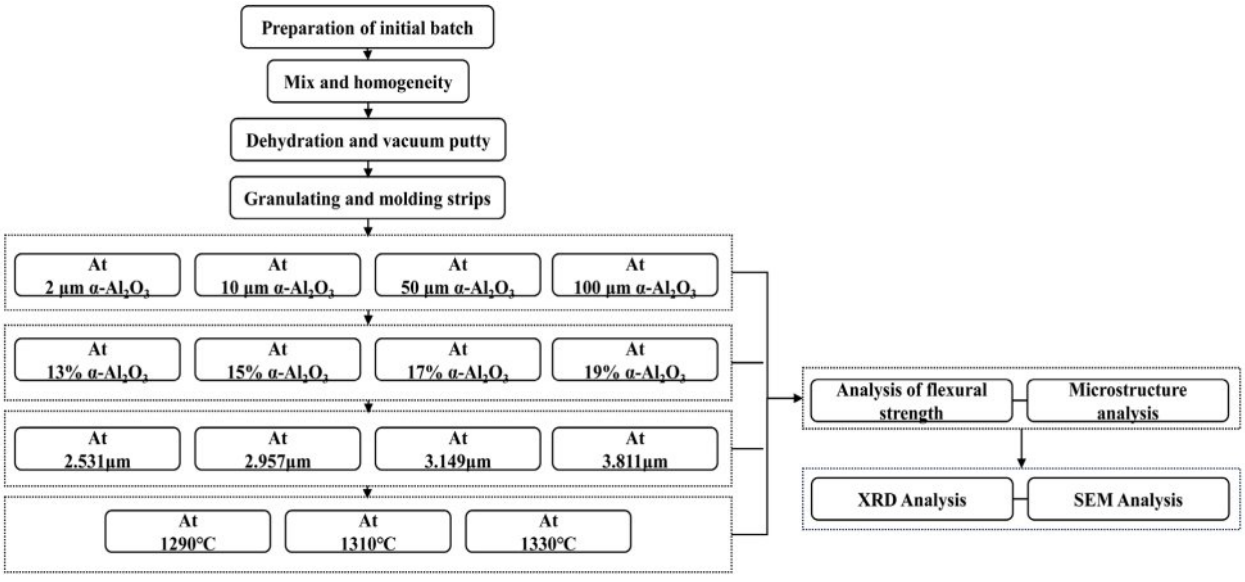

Fig. 1. Flowchart of the experimental procedure.

Table 1. Chemical composition of raw materials (wt%).

	Na_2O	MgO	Al_2O_3	SiO_2	K_2O	CaO	TiO_2	MnO	Fe_2O_3
Baoxi Clay	0.10	0.06	15.75	73.91	5.50	0.03	0.05	0.06	0.87
Feldspar	2.70	0.09	16.40	69.32	9.79	0.52	0.02	0.00	0.10
Malaysia Kaolin	0.02	0.09	36.40	49.68	0.37	0.04	0.02	0.00	0.08
bentonite	3.27	5.35	14.11	69.63	2.16	2.67	0.14	1.68	3.27
α-Al_2O_3	α-$Al_2O_3 \geq 99.9\%$								

EDS analysis was conducted utilizing an IXRF Model 550i energy spectrometer.

Finally, the phase composition and other characteristics of the ceramic body's surface post-etching were assessed using an X-ray diffractometer (D8 Advance, Bruker AXS GmbH, Germany).

Results and Discussion

Effect of α-Al_2O_3 Particle Size on the Flexural Strength of Celadon Bodies

According to prior research findings and theoretical models [20-22], the properties of most ceramic bodies are often intricately linked to their microstructure. This study investigates the influence of α-Al_2O_3 particle size on the flexural strength of Longquan celadon bodies, accompanied by a comprehensive analysis of experimental data. From the results presented in Fig. 2, it can be deduced that within a specific range, an increase in α-Al_2O_3 particle size initially enhances the flexural strength of the celadon body, before ultimately leading to a decline. Specifically, at a particle size of 10 μm, samples demonstrate peak flexural strength with an average value of 104.1 MPa, approximately 92% higher than that observed in celadon bodies devoid of α-Al_2O_3. However, as the particle size continues to rise beyond this threshold, there is a marked reduction in flexural strength; this phenomenon may be attributed to modifications in microstructure.

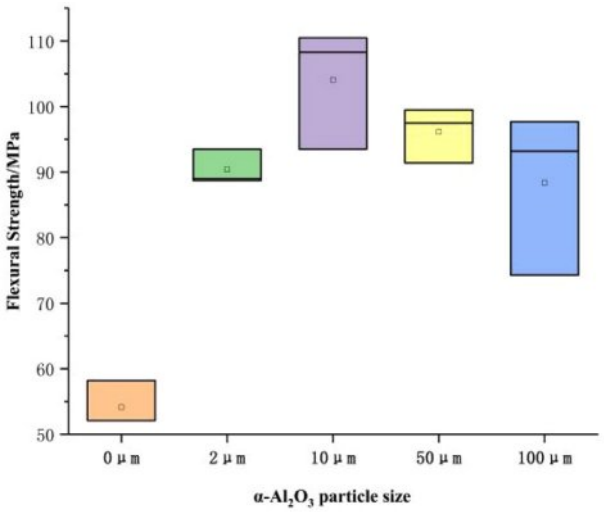

Fig. 2. Influence of α-Al_2O_3 particle size on flexure strength.

When the particle size of α-Al_2O_3 is reduced, smaller particles can be more effectively dispersed within the matrix. This enhanced dispersion facilitates dispersion toughening and significantly impedes crack propagation during sintering. Such improvements lead to increased

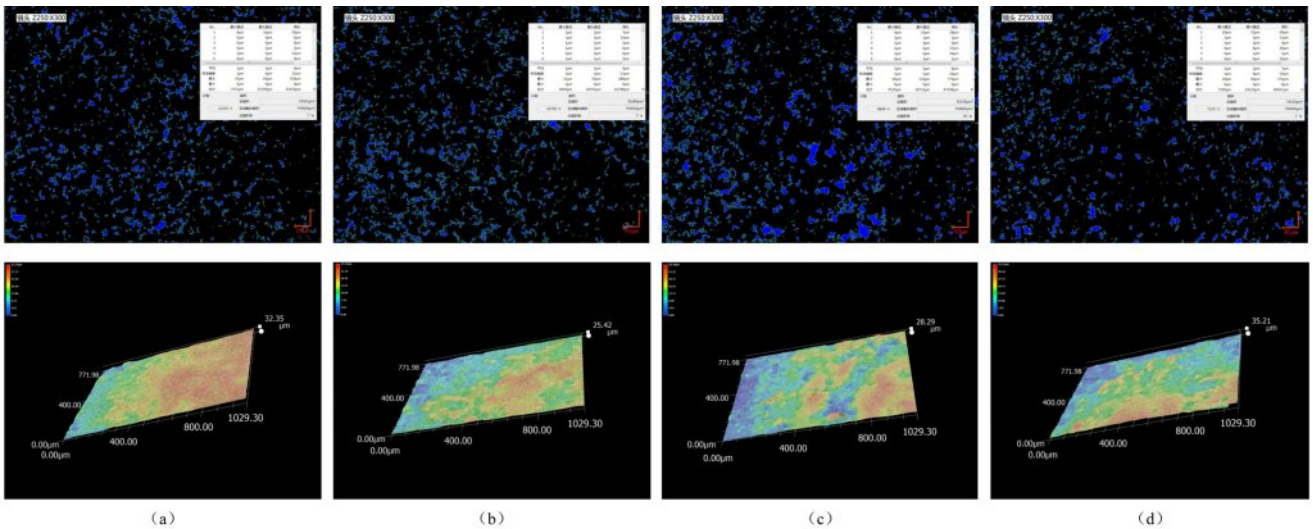

Fig. 3. Two-dimensional and three-dimensional morphologies of the matrix surface of different samples: (a) 2 μm; (b) 10 μm; (c) 50 μm; (d) 100 μm.

toughness and bending resistance of the material. Additionally, a smaller particle size of α-Al_2O_3 promotes the formation of mullite crystals, which exhibit greater strength and hardness, thereby further increasing the flexural strength of the composite material. Moreover, α-Al_2O_3 establishes strong chemical bonds with other components in the celadon body, enhancing the overall strength of the material. Conversely, incorporating larger-sized α-Al_2O_3 particles into the celadon body results in decreased grain boundaries within the sample due to their chemical interaction with other constituents. This reduction adversely affects its flexural properties and ultimately leads to a decline in flexural strength. Microscopic observations conducted using an ultra-depth-of-field microscope (Fig. 3) illustrate that as particle size of α-Al_2O_3 continues to increase, incomplete reactions among raw materials occur. Consequently, this phenomenon induces structural defects within the sample and results in a rough surface texture characterized by heightened porosity throughout the body.

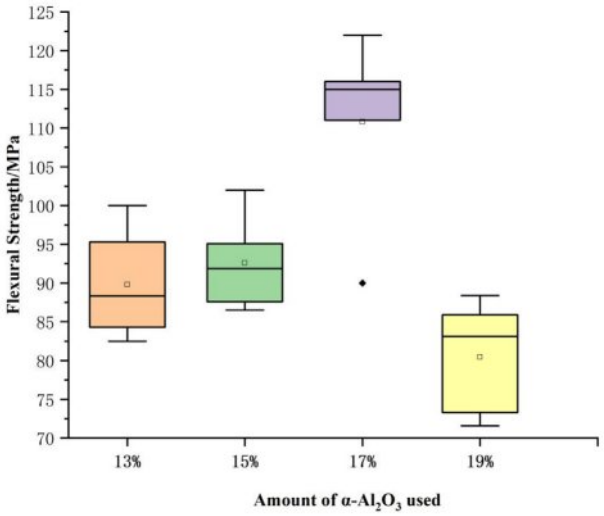

Fig. 4. Influence of α-Al_2O_3 usage amount on flexure strength.

Effect of α-Al_2O_3 content on the Flexural Strength of Celadon Bodies

In previous studies, it has been demonstrated that α-Al_2O_3 with a particle size of 10 μm provides the most significant enhancement in the flexural strength of Longquan celadon bodies. Building upon these findings, this study further investigates the effect of varying α-Al_2O_3 content on the bending strength of Longquan celadon. During the experimental process, quantities of 13%, 15%, 17%, and 19% by weight of 10 μm α-Al_2O_3 were incorporated into the base formulation. The mixture underwent ball milling for eight hours to prepare samples, which were subsequently fired at a temperature of 1310 °C under reducing conditions.

Fig. 4 illustrates that the flexural strength of Longquan celadon body initially increases with rising α-Al_2O_3 content, ultimately reaching a peak before decreasing. Specifically, when the α-Al_2O_3 content reaches 17%, the maximum recorded flexural strength averages at 110.8 MPa, The results indicate an approximate 104% increase in flexural strength compared to the body without α-Al_2O_3. This finding highlights that augmenting the amount of α-Al_2O_3 within a specific range can significantly enhance the flexural strength of the body. This phenomenon can be attributed to the introduction of a small quantity of α-Al_2O_3, which is uniformly dispersed throughout the material and remains inert during preparation, thus facilitating dispersion strengthening. As a result, this contributes to improved sintering and densification within the body, ultimately leading to enhanced flexural strength. However, α-Al_2O_3 surpasses a certain concentration threshold, it begins reacting with SiO_2 to form mullite crystals. This results in a composite structure characterized by evenly distributed α-Al_2O_3

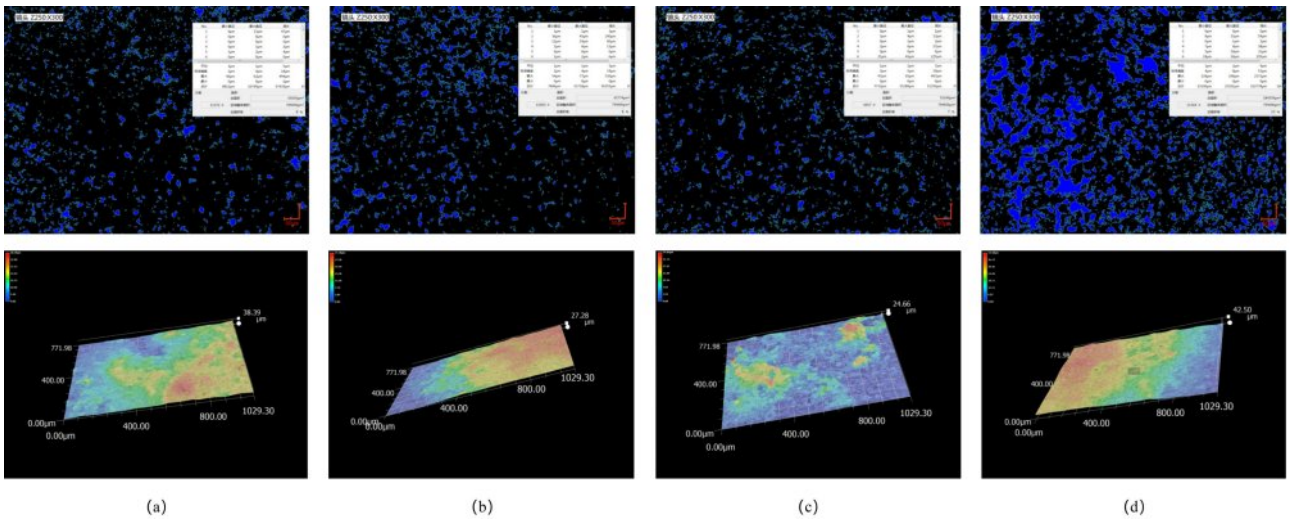

Fig. 5. Two-dimensional and three-dimensional morphologies of the matrix surface of different samples: (a) 13%; (B) 15%; (C) 17%; (d) 19%

particles alongside an extensive network of elongated mullite phases at grain boundaries or interfaces. Such formations hinder crack propagation induced by stress application, thereby enhancing both compactness and bending strength. As further increments in α-Al_2O_3 occur beyond this point, aggregation within the body leads to larger mullite crystal phases; this transition ultimately elevates porosity levels within the material. Additionally, elevated concentrations of α-Al_2O_3 enhance refractoriness but may contribute to underfiring issues within the matrix—resulting in significant reductions in overall structural integrity [23]. Moreover, it should be noted that introducing α-Al_2O_3 may also instigate chemical reactions or physical adsorption with other components present in the substrate; these interactions can significantly influence both structure and properties. These interactions contribute to the enhancement of the flexural strength of the body when the introduction amount is within an appropriate range. However, excessive amounts can have detrimental effects, leading to a reduction in flexural strength. Observations made using an ultra-depth microscope, as illustrated in Fig. 5, reveal that with increasing α-Al_2O_3 introduction levels, there is an improvement in the sintering degree of the body and a corresponding decrease in surface roughness. Nevertheless, as the introduction amount approaches 19%, there is an observed increase in both surface roughness and porosity, which consequently results in a decline in the flexural strength of the body [24].

Effect of medium diameter on the Flexural Strength of Celadon Bodies

By optimizing the particle size of the raw material through refinement, a significant enhancement in the flexural strength of the final product can be attained. This principle is supported by extensive research theories [25, 26]. By precisely controlling both milling time and efficiency, use a laser particle size analyzer to test and analyze the median diameter of the raw material, median diameters (D50) of the raw material were established at 2.531 μm, 2.957 μm, 3.149 μm, and 3.811 μm respectively. This methodology seeks to investigate the influence of varying median diameters on the flexural strength of Longquan celadon bodies.

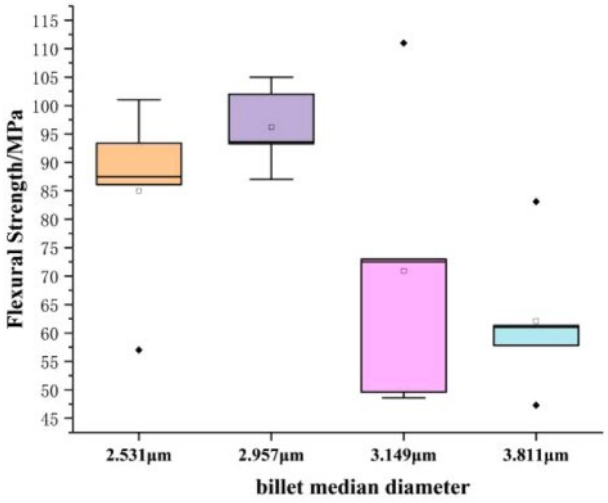

Fig. 6. Influence of billet median diameter on flexural strength.

It can be observed from Fig. 6 that the flexural strength of Longquan celadon samples exhibits a distinct trend in relation to the median diameter (D50) of the raw ceramic material. Initially, the flexural strength increases and then subsequently decreases. When the median diameter D50 is 2.957 μm, the sample achieves its maximum flexural strength with an average value of 94.725 MPa. These results indicate that an optimal median diameter D50 for the raw material plays a crucial role in both the sintering and densification processes of Longquan celadon.When D50 is small, finer grain sizes are present within the

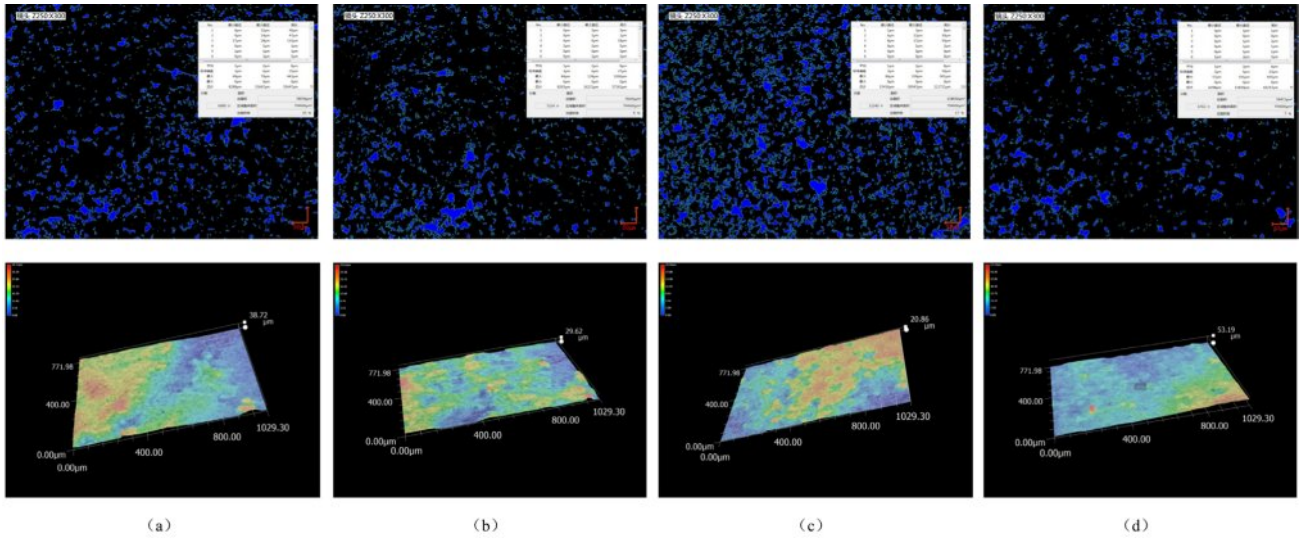

Fig. 7. Two-dimensional and three-dimensional morphology of ceramic body of different samples surfaces: D50=2.531 μm, (b) D50=2.957 μm, (c) D50=3.149 μm, (d) D50=3.811 μm.

body, which facilitates sintering and densification—thereby enhancing its flexural strength. This enhancement occurs because a finer particle distribution allows for more thorough reactions among raw materials, increases atomic activity, and accelerates diffusion rates along grain boundaries; however, at this stage, these grain boundaries exhibit certain viscosity levels that diminish their ability to resist deformation, ultimately improving overall performance [27].

Conversely, when D50 increases, coarser particles result in uneven sintering within the body, leading to an increase in porosity. Moreover, larger particle distributions contribute to incomplete reactions among raw materials; consequently, this diminishes the performance of the body and reduces its flexural strength. The microscopic surface characteristics of the blank body were analyzed using a superfield microscope as illustrated in Fig. 7. As D50 continues to rise, there is a marked decline in the degree of sintering while surface roughness progressively increases alongside heightened porosity levels.

Effect of firing temperature on the Flexural Strength of Celadon Bodies

According to the analysis presented above, the flexural strength of the ceramic body is significantly enhanced when 10 μm α-Al_2O_3 is incorporated at a concentration of 17%, with the median diameter of the raw material measured at 2.957 μm. Furthermore, this study investigates the effects of reduction firing conducted at temperatures of 1290 °C, 1310 °C, and 1330 °C on the properties of Longquan celadon bodies [28].

As illustrated in Figs. 8 and 9, the porosity of the body

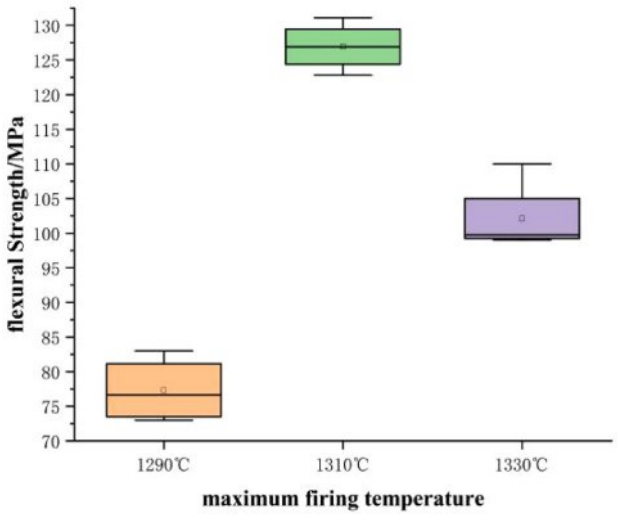

Fig. 8. Influence of maximum firing temperature on flexural strength.

varies with changes in firing temperature, leading to a trend where flexural strength initially increases and then decreases. This phenomenon can primarily be attributed to several factors: First, at lower sintering temperatures, α-Al_2O_3 reacts with SiO_2 within the body to form mullite crystals. This reaction not only reduces the content of free SiO_2 but also mitigates volume change defects arising from the polycrystalline transformation of SiO_2 due to temperature fluctuations, thereby enhancing the strength of the body during firing. Secondly, as sintering temperature increases, the degree of sintering deepens gradually. The emergence of a liquid phase

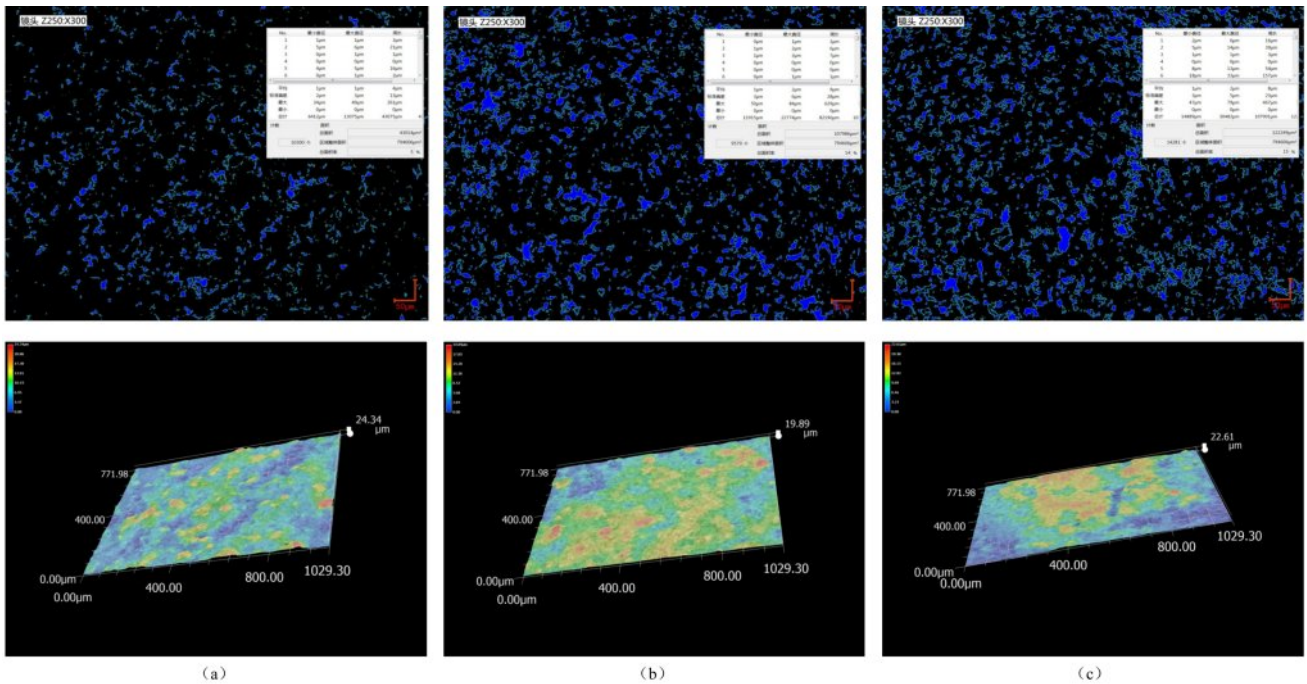

Fig. 9. Two-dimensional and three-dimensional morphologies of the body surface of different samples: (a) 1290 °C; (B) 1310 °C; (C) 1330 °C.

facilitates partial dissolution and reactions that yield an eutectic mixture which further reduces sample porosity and enhances modal density. Together, these effects contribute to a continuous increase in flexural strength.

At a reduction and sintering temperature of 1310 °C, the sample achieves optimal performance with an average flexural strength of 126.9 MPa—an approximate increase of 134% compared to unoptimized bodies. At this relatively appropriate temperature, the mullite crystals have moderate size and uniform distribution, which can form a good reinforcement effect in ceramic materials. However, if the firing temperature continues to increase beyond this temperature, the body begins to experience over-firing, with the porosity gradually increasing, which may lead to excessive crystal growth and oversized dimensions, making the distribution of the reinforcing phase uneven, causing the body structure to become unstable, increasing the brittleness of the material, and resulting in unsatisfactory strength improvement effect. On the contrary, if the temperature is too low, the mullite crystals are small and unevenly distributed, making it difficult to exert an effective reinforcement effect [29].

In order to further elucidate the effect of α-Al_2O_3 on the flexural strength of Longquan celadon, optimal parameters were selected for sample preparation. The particle size of α-Al_2O_3 is 10 μm, with a content of 17%. The median diameter (D50) of the slurry measures 2.957 μm, and the maximum sintering temperature reaches 1310 °C. Following the bending strength tests, an analysis of the fracture surface was conducted using SEM, EDS, and XRD techniques.

Figure 10 illustrates a distinct microstructure characterized by overlapping granular corundum and acicular mullite within the cross-section of the sample; numerous dimples are also present. The formation process of these dimples encompasses stages such as micropore creation, growth, and interconnection. The presence of these dimples can alter the distribution of stress, alleviating the concentration of internal stress produced during the preparation or use of porcelain, allowing the porcelain to more evenly disperse stress when under force, thus improving the toughness of porcelain [30]. At the same time, there are cleavage steps (indicated by arrows) accompanied by a small amount of intergranular fracture microcracks, indicating that there are no significant defects in the structure of the sample, showing better bending strength. When the distribution of pits can present a certain degree of non-uniformity on a microscopic scale without compromising the overall structural integrity of the material, this non-uniformity can prevent cracks from rapidly and continuously expanding within the material, thus improving the material's

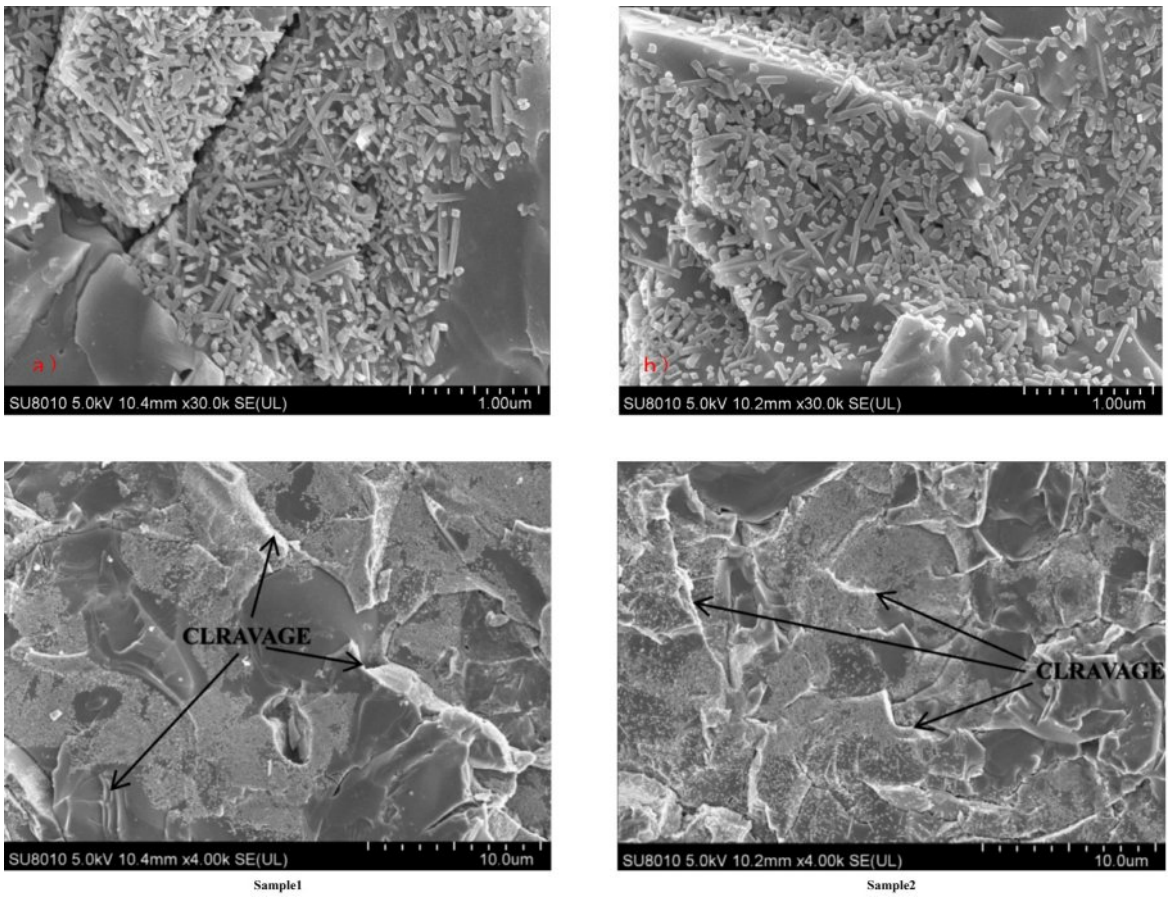

Fig. 10. SEM image of sample section under optimized parameters,

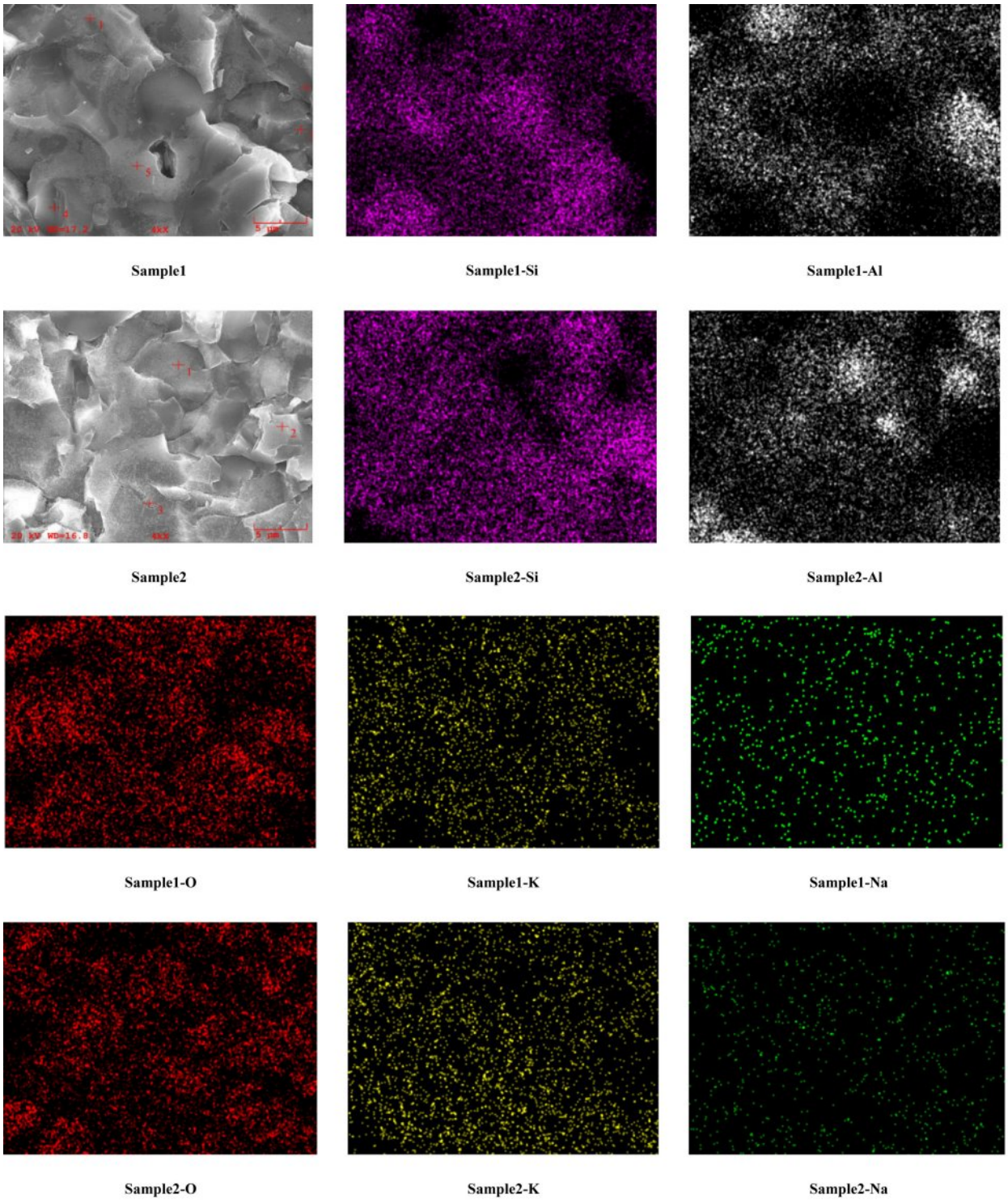

Fig. 11. SEM photos and element distribution map of the sample section under the optimized parameters,

resistance to crack propagation [18]. Examination of the fracture surface reveals that acicular mullite and granular corundum coexist in a network structure which effectively impedes grain boundary sliding and crack propagation. This arrangement mitigates any detrimental effects typically associated with high elastic modulus corundum on impact strength while simultaneously enhancing overall toughness. As a result, this leads to a stable and high-strength Longquan celadon body.

Figure 11 illustrates the element distribution map of the sample section under optimized parameters. In conjunction with the EDS analysis results presented in Table 2, the primary element distributions for samples 1# and 3# of Sample 1 are observed to be Al and O. For

Table 2. EDS analysis results of samples with better paramters.

	Sample 1(Conc./wt%)					Sample 2(Conc./wt%)		
	1#	2#	3#	4#	5#	1#	2#	3#
O	40.656	33.286	42.173	45.704	42.848	38.093	47.850	40.246
Na	0.891	1.292	0.990	-	-	-	1.276	1.542
Al	51.135	12.174	51.025	4.681	20.223	51.368	4.579	13.480
Si	6.104	46.444	4.731	46.649	31.757	10.539	44.087	37.618
K	1.214	6.805	1.082	2.966	5.171	-	2.208	7.114

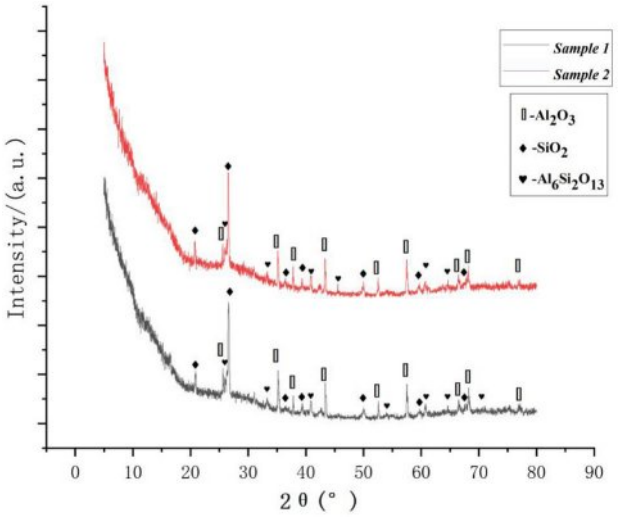

Fig. 12. XRD pattern of samples with better parameters.

samples 2# and 5#, the predominant elements include Al, Si, and O, while point 4 predominantly features Si and O. In Sample 2, Element distribution is as follows: at location 1#, primarily Al and O are identified; at location 2#, Si and O dominate; and at location 3#, a combination of Al, Si, and O is noted. Both samples contain a significant amount of alkaline oxides.

Combined with the in-depth analysis of the X-ray diffraction (XRD) pattern of the sample, as shown in Fig. 12, it is possible to determine the characteristics of the sample prepared under a specific α-Al_2O_3 addition method and firing temperature. The sample is primarily composed of corundum phase (α-Al_2O_3), quartz phase (SiO_2), and mullite phase ($Al_6Si_2O_{13}$). In contrast, traditional ceramics mainly comprise mullite phase, quartz phase, and glass phase, with minimal corundum presence. The formation of these crystalline phases has resulted in a further enhancement of the flexural strength of the samples. Consequently, by controlling both the addition form of α-Al_2O_3 and the firing temperature, it is feasible to prepare a sample characterized by stable corundum and mullite phases. This approach facilitates the development of a microstructure that exhibits no apparent defects, thus ensuring excellent physical properties such as bending strength and other related attributes [31].

Conclusion

This study conducted experimental research on the relationship between the flexural strength of Longquan celadon body and different process parameters. It is found that the flexural strength of Longquan celadon body can be effectively improved by adjusting and optimizing the process parameters such as the particle size of α-Al_2O_3, the amount of α-Al_2O_3, the median diameter D50 of the raw material of body and the firing temperature. The Experimental results show that the flexural strength of the body compacts increases with the increase of α-Al_2O_3 particle size and the amount of α-Al_2O_3 in a certain range. When 10 μm of α-Al_2O_3 and 17% of α-Al_2O_3 were selected, the mean flexural strength of the body reached a stable extreme value of 126.9 MPa when the median diameter of the raw material reached 2.957 μm and the body was sintered at 1310 ℃ in reducing atmosphere. The results of SEM, EDS and XRD show that the body structure is more compact, and there are corundum phase, quartz phase and mullite phase, and there are more dimples and cleavage steps on the fracture surface under the optimal parameters, which makes the sample matrix have good toughness and high flexural strength.

The body formula of Longquan celadon was optimized and prepared. These results provide a useful reference for improving the preparation process and material formula of Longquan celadon. Future research directions include exploring the effects of other process parameters on the flexural strength and analyzing the formation mechanism of various phases in the body, and pointing out the direction for further improving its performance.

Declaration of Competing Interest

The authors declare that they have no known competing financial interests or personal relationships that could have appeared to influence the work reported in this paper.

Acknowledgment

This study was supported by the Longquan Science and Technology Bureau's "Industrialization Technology

Research on High-Alumina-Mullite-Quality Longquan Strengthened Porcelain" and the Jingdezhen Science and Technology Bureau's Science and Technology Plan Project (20234SF001).

References

1. R. Zhou, in “Research on Celadon of Longquan” (Cultural Relics Publishing House, 1998).
2. J.Z. Li, in “History of Science and Technology in China - Ceramic Volume” (Science Press, 1998).
3. Q. Shi and X.P. Ye, Kuei Suan Yen T'ung Pao. 36[8] (2016) 2460-2465.
4. S.M. Zhou, X.G. Ding, and H.M. Ye, T'ao Tz'u Hsueh Pao. 31[1] (2010) 170-175.
5. Y.F. Lin, Y.L. Jin, and J.F. Jin, Art Education Research. 15 (2015) 46-47.
6. Y.Y. Guo, S.Y. Wang, and Y.C. Chen, Kuei Suan Yen T'ung Pao. 12[3] (1980) 232-243.
7. J. Wu, P. Jiang, Q.J. Li, J.M. Wu, and M.L. Zhang, Chung-kuo T'ao Tz'u. 52[11] (2016) 53-57.
8. Z.C. Mao and W.J. Mao, Chung-kuo T'ao Tz'u Kung Yeh. 41[3] (2017) 12-15.
9. Y. Shen and L.S. Liu, Chung-kuo T'ao Tz'u. 35[01] (2000) 1-3.
10. P. Wimuktitwan, M. Rodchom, K. Soongprasitt, U. Atong, and S. Vichaphund, Ceram.-Silik. 64[2] (2020) 164-171.
11. D. Hao, T. Akatsu, and N. Kamochi, J. Ceram. Soc. Jpn. 128[4] (2020) 194-200.
12. X.H. Zhang, J.H. Zhang, and C.X. Liu, Shan-tung Ta Hsueh Hsueh Pao, Kung Hsueh Pan. 34[5] (2004) 14-17.
13. H.M. Ye, H. Yang, and J.J. Lu, T'ao Tz'u Hsueh Pao. 26[1] (2005) 7-12.
14. H.X. Qu, S. Zhu, W.S. Gu, Q. Li, and C.X. Ouyang, J. Ceram. Process. Res. 14[3] (2013) 363-370.
15. A. Akkus and T. Boyraz, J. Ceram. Process. Res. 20[1] (2019) 54-58.
16. Z.F. Chu, C.Y. Jia, J.C. Liu, R. Ding, and A. Zhang, J. Ceram. Process. Res. 18[2] (2017) 122-126.
17. W. Chen, in “Microstructure Evolution and Its Regulation During α-Al_2O_3 Formation” (Central South University, 2010).
18. D.D. Zhao, J. Ceram. Process. Res. 25[5] (2024) 910-917.
19. H.W. Choi, S.J. Kim, H. Yang, Y.S. Yang, Y.H. Rim, and C.R. Cho, J. Ceram. Process. Res. 20[1] (2019) 63-68.
20. Y.T. Shao, J.H. Yu, S.B. Wu, J.J. Lan, X.P. Ye, and Y.F. Wu, Journal of Lishui University. 24[2] (2022) 28-36.
21. Y.F. Wu, J.H. Yu, L.L. Mei, et al., T'ao Tz'u Hsueh Pao. 42[3] (2021) 458-465.
22. Q.F. Bao, W.X. Dong, J.E. Zhou, and Y.Z. Wang, Chung-kuo T'ao Tz'u. 43[3] (2014) 39-41.
23. B. Peng, in “Research on Celadon Technology of Longquan” (Zhejiang University, 2010).
24. D.C. Kim and S.G. Kang, J. Ceram. Process. Res. 24[6] (2023) 926-934.
25. S.Z. Chavoshi, P.S. Branicio, and A. Qi, Phys. Rev. Mater. 5[7] (2021).
26. R. Rui, J.F. Jianfeng, B.S. Wang, et al., J. Alloys Compd. 920 (2022) 1-7.
27. D.K. He, in “Research on Particle Dispersion Prestressed Reinforced Domestic Ceramics” (Jingdezhen: Jingdezhen Ceramic University, 2023).
28. A. Rittidech and A. Suthapintu, J. Ceram. Process. Res. 25[1] (2024) 22-27.
29. Z.F. Chen, S.F. Zhu, Q.Q. Wang, and X.B. Wang, J. Ceram. Process. Res. 25[1] (2024) 56-64.
30. B. Lu, in “In-Situ Synthesis of Particle Reinforced Aluminum Matrix Composites and Their Mechanical Properties” (Shaanxi University of Science and Technology, 2019).
31. U. Önen and T. Boyraz, J. Ceram. Process. Res. 25[4] (2024) 624-632.